JOURNAL OF MATERIALS SCIENCE 25 (1990) 2737–2742

Segregant-enhanced fracture in magnesium oxide

C. L. CONNER
Department of Ceramic Engineering, The Ohio State University, Columbus, Ohio 43210, USA
K. T. FABER
Department of Materials Science and Engineering, Northwestern University, Evanston, Illinois 60208, USA

The fracture toughness of MgO has been studied as a function of the concentration of an intergranular LiF phase, added to enhance densification. The fracture toughness increases as lithium and fluorine are volatilized from the MgO while the fracture morphology changes from intergranular to transgranular. The data are interpreted with respect to competing embrittlement and crack-deflection toughening mechanisms, and a scheme is proposed for determining conditions for embrittlement and toughening.

1. Introduction

In polycrystalline ceramic materials, grain boundaries and their associated impurities can significantly influence the fracture behaviour. Impurities may result from a variety of sources: impure starting materials, processing techniques, or often from deliberate additions to aid sintering by promoting solid-state diffusion or by forming a liquid phase. These impurities may then segregate to the grain boundaries resulting in enhanced impurity levels or, in the case of sintering aids, may remain at boundaries to form a residual amorphous grain boundary phase. The grain boundary region comprised of segregated impurities or a second phase may be accompanied by residual strains and is likely to differ in fracture toughness from the grain itself. A grain boundary toughness which is less than that of the bulk grain leads to intergranular fracture, resulting in embrittlement in many metals and metallic compounds [1, 2]. For ceramics, the situation is more complex and fracture via the grain boundaries may result in embrittlement or, alternatively, in toughening due to crack deflection as reviewed herein.

Grain-boundary impurity segregation has been well documented in ceramics [3–8]. In particular, the segregation of calcium in Al_2O_3 has been noted by a number of investigators [6–8]. However, only two studies relate the impurity concentration and segregation to the fracture toughness of Al_2O_3 [9, 10]. Most noteworthy are the observations of Jupp *et al.* [9] who reported an inverse relationship between the fracture toughness and the amount of calcium segregation along Al_2O_3 grain boundaries. Alumina containing non-detectable levels of calcium demonstrated transgranular fracture and the highest fracture toughness. The toughness decreased as the amount of grain boundary calcium and the percentage of intergranular fracture increased. Similarly, Evans *et al.* [11] concluded that "cleaner" grain boundaries in MgO result in a larger effective surface energy for fracture, making crack extension more difficult. Other studies of MgO containing lithium fluoride, carbonate, and hydroxl ions have indirectly evidenced the embrittling effects of grain boundary impurities in strength, rather than toughness measurements [12].

Grain boundary or intergranular fracture, however, need not be deleterious to the toughness of a ceramic material compared to transgranular fracture. Possible toughening arises when the crack driving force for a non-planar crack is reduced due to mixed-mode loading. As a crack grows along a grain boundary, it tilts and twists out of the plane perpendicular to the applied loading. These tilted and twisted portions of the crack front are subject to mixed-mode loading and can be characterized by their local stress intensities k_1, k_2, and k_3. The change in crack driving force is then evaluated by averaging over the local stress intensities at the tilted and twisted portions of the crack front [13]. Crack advance is assumed to be governed by the change in strain energy release rate, $\mathcal{G}$, for each segment of the crack front along its deflected trajectory:

$$E\mathcal{G} = k_1^2(1 - \nu^2) + k_2^2(1 - \nu^2) + k_3^2(1 + \nu) \quad (1)$$

where E and ν are Young's modulus and Poisson's ratio, respectively. The average strain energy release rate across the crack front $\langle\mathcal{G}\rangle$ is then considered to be the net driving force. A comparison of $\langle\mathcal{G}\rangle$ with the corresponding strain energy release rate of the undeflected or planar crack, $\mathcal{G}^{\text{planar}}$, provides the basis for predicting the toughening increment, $\mathcal{G}_c$ [13]:

$$\mathcal{G}_c = \mathcal{G}_c^{\text{planar}}\,[\mathcal{G}^{\text{planar}}/\langle\mathcal{G}\rangle] \quad (2)$$

Equation 2 assumes that the toughness of the deflected path is equivalent to the material in the plane, an assumption that is not appropriate for grain boundary failure and will be addressed in a subsequent section. However, in all cases, the driving force for a

0022–2461/90 $03.00 + .12

non-planar crack is less than that for a planar crack oriented normal to the applied stress. Hence, toughening may occur provided that the toughness of the grain boundary phase is not significantly different from the toughness of the grain.

A number of materials have demonstrated that fracture along grain boundary phases can provide toughening. Toughening via crack deflection is exhibited in SiC containing minor Al_2O_3 additions [14] and in ferrites having an intergranular insulating phase [15]. Strength increases have also been observed in MgO having minor cation impurity additions [12] and as a consequence of grain boundary precipitates in magnesium–aluminium spinel [16] and wustite [17]. In each of these cases, the relative toughness of the grain boundary compared with the grain is expected to control the fracture path, as well as determine whether embrittlement or crack-deflection toughening occurs.

In our research, magnesium oxide is used as a model material to investigate the effects of grain boundary impurities on fracture toughness. By heat treatment, the grain boundary composition is altered and direct measurements of fracture toughness are made to determine which mechanism, embrittlement or crack deflection toughening, is operative. We propose a scheme of analysing the grain boundary toughness and the conditions for establishing embrittlement and toughening.

2. Experimental procedure

The fully-dense, transparent MgO used in this research (courtesy of T. Vasilos, AVCO Corp.) was hot-pressed using LiF as a sintering aid. The procedure for fabrication of this MgO has been described by Rice [18] and Miles *et al.* [19]. Initially 1 to 2 mol % LiF was added to the MgO, with a maximum of 0.5% remaining after hot-pressing. Transparency was achieved through a post-pressing heat treatment to volatilize the LiF. The final transparent MgO contained a residual amount of LiF (0.05 to 0.1%). It has been postulated that the remaining LiF is present as a thin film at the grain boundaries [20, 21]. For this research, MgO specimens were subjected to further heat treatments to remove any remaining LiF. Samples were heated in air at a rate of $48^\circ C\,h^{-1}$ to temperatures of 950, 1100, 1250 and 1400° C and held at temperature for 30 min. A second cycle to 1400° C was also conducted.

Fracture toughness was measured for specimens heat-treated at each temperature by indentation strength-in-bending (ISB) [22] using 0.42 cm × 0.32 cm × 2.54 cm bend bars. Vickers indentations were made with loads of 15 to 30 N, oriented such that one set of orthogonal cracks was perpendicular to the tensile stress axis. Bars were tested in three-point bending at a stressing rate of $135\,MPa\,sec^{-1}$. The hardness-to-modulus ratio, necessary to compute the fracture toughness using the ISB method, was determined from Knoop indentation impressions [23].

Fracture surfaces were examined by scanning electron microscopy (SEM) to confirm that failure occurred at the indentation, to determine the mode of fracture, and to examine grain boundary microstructure. The bulk lithium content was measured by atomic absorption spectroscopy and the bulk fluorine concentration by selective electrode analysis. A scanning Auger microprobe (SAM) was used to analyse grain boundary segregants.

3. Results

Fracture toughness as a function of heat-treatment temperature is shown in Fig. 1. Fracture toughness values are normalized to the measured fracture toughness K_{Ic} of $2.2\,MPa\,m^{1/2}$ for the as-received material. Through the 1100° C heat treatment there is no significant change in fracture toughness. Heat treatments above 1250° C result in an increase in fracture toughness, with values up to 30% greater ($2.9\,MPa\,m^{1/2}$) than the as-received material achieved after the 1400° C treatment. SEM evaluation of the fracture surfaces shows a corresponding change in mode of fracture. Fig. 2 is a series of SEM micrographs of the fracture surfaces associated with each heat treatment. The as-received MgO and that heat-treated at 950 and 1100° C exhibit nearly 100% intergranular fracture (Fig. 2a). As the heat-treatment temperature is increased, transgranular fracture is observed (Fig. 2b). By the final heat treatment, with the highest K_{Ic}, the fracture mode is approximately 40% transgranular (Fig. 2c). The heat treatments did result in minor grain growth. The as-received material has an average grain size of 25 μm. After the 1400° C treatment, the average grain size increases to 35 μm.

The results of the bulk chemical analyses for lithium and fluorine are shown in Fig. 3. In the as-received material, the lithium and fluorine concentrations did not correspond to stoichiometric LiF. This non-simultaneous volatilization of LiF was also seen by Haussonne *et al.* [24] in the removal of LiF from barium titanate. Johnson *et al.* [25] also observed low levels of lithium and greater retention of fluorine after the hot-pressing of MgO. The heat treatments for this research resulted in further loss of both lithium and fluorine, but at different rates. Lithium was lost at a fairly constant rate to a total loss of 17%. The fluorine reached a final loss of 60% but 40% of the fluorine was lost by the 950° C heat treatment. At all heat-treatment temperatures, there is an excess of fluorine compared to stoichiometric LiF. A scanning Auger microprobe profile across a grain and grain boundaries of a material heat-treated at 1400° C showed fluorine

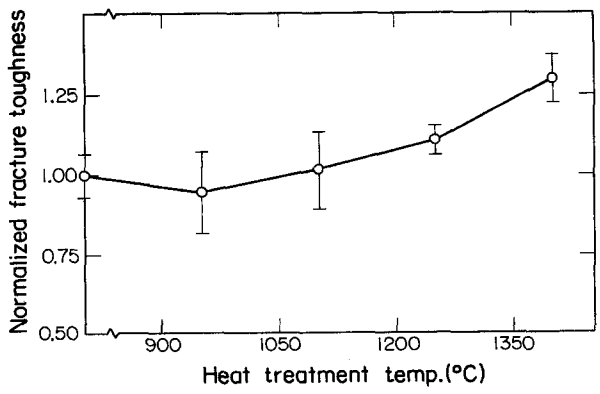

Figure 1 Fracture toughness of MgO hot-pressed with LiF measured as a function of heat-treatment temperature.

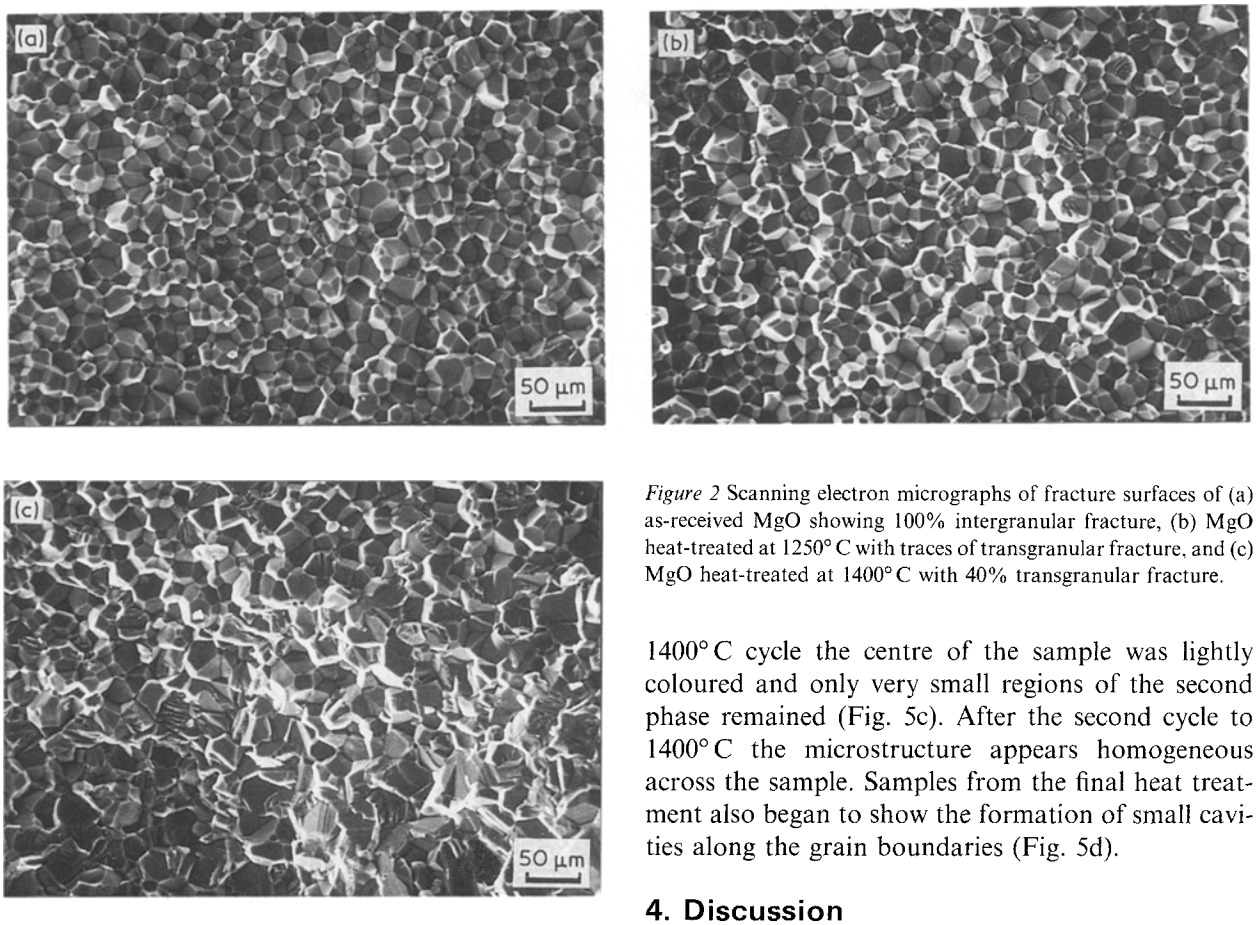

Figure 2 Scanning electron micrographs of fracture surfaces of (a) as-received MgO showing 100% intergranular fracture, (b) MgO heat-treated at 1250° C with traces of transgranular fracture, and (c) MgO heat-treated at 1400° C with 40% transgranular fracture.

only at or near the grain boundaries, not in the centre of the grain (Fig. 4).

The colour of the samples underwent a dramatic change through the heat treatments. Initially, the as-received MgO is colourless. The colour changed from a faint red-orange after the 950° C treatment to dark brown at 1250° C. Heat treatment to 1400° C resulted in a loss of colour. In all cases, the samples retained their transparency. These colour changes are associated with the change in valence of manganese ions present as impurities in the starting powder [19, 26, 27].

The presence of a second phase at the grain boundary was confirmed by the SEM analysis. In the as-received MgO the second phase was a continuous film, approximately 0.25 to 0.50 μm thick, completely wetting the grain boundaries as seen in the SEM micrograph in Fig. 5a. As the samples were heat-treated and lithium and fluorine lost, the second phase broke up into isolated spheres at 1250° C (Fig 5b). After the first 1400° C cycle the centre of the sample was lightly coloured and only very small regions of the second phase remained (Fig. 5c). After the second cycle to 1400° C the microstructure appears homogeneous across the sample. Samples from the final heat treatment also began to show the formation of small cavities along the grain boundaries (Fig. 5d).

4. Discussion

The change in fracture toughness and mode of fracture of MgO can be correlated with the presence and properties of the lithium- and fluorine-enhanced boundary phase. The samples having a continuous grain-boundary phase exhibited nearly 100% intergranular fracture and the lowest fracture toughness. Conversely, the toughest sample evidenced approximately 40% transgranular fracture. As the grain boundary was altered by the removal of lithium and fluorine and by the corresponding break-up of the continuous phase, the fracture toughness increased and the mode of fracture changed from intergranular to transgranular.

The controlling factor for the fracture toughness of the LiF-fluxed MgO is the toughness of the grain boundary, K_{Ic}^{b}, relative to the toughness of the grain, K_{Ic}^{g}. If $K_{Ic}^{b} < K_{Ic}^{g}$, the likely path for fracture is the grain boundary. This inequality, however, is not sufficient for embrittlement of the polycrystal to occur. To assess the conditions for embrittlement, recall

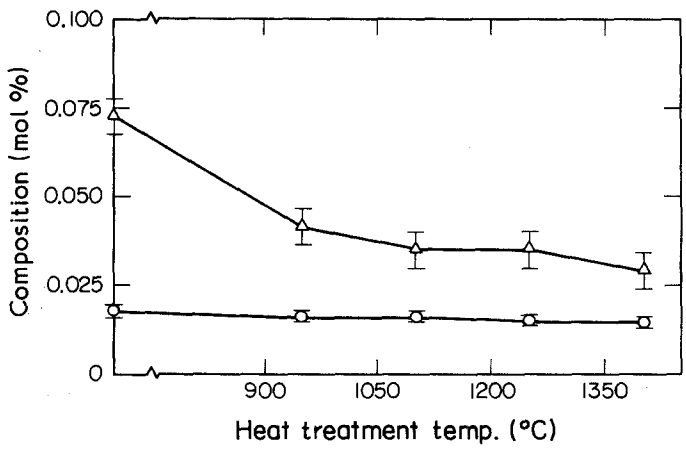

Figure 3 Chemical analyses of (○) lithium and (△) fluorine as a function of heat-treatment temperature.

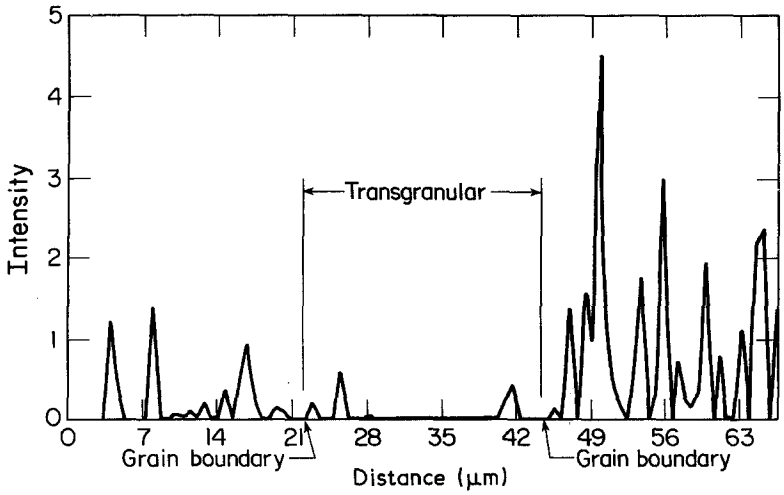

Figure 4 Scanning Auger microprobe scan of fluorine across fracture surface of MgO heat-treated at 1400° C. Regions of intergranular failure exhibit enhanced fluorine content, while fracture across grains shows little or no fluorine.

Equation 2 for the critical strain energy release rate, $\mathcal{G}_c$, for a non-planar crack [13]. The ratio $\langle\mathcal{G}\rangle/\mathcal{G}^{planar}$ has been calculated as a function of grain morphology, and hence crack plane topography, and plotted in Fig. 6. Intergranular fracture of equiaxed grains would demonstrate a driving force approximately 75% of that of a planar crack, while the driving force for a crack propagating around elongated grains having an aspect ratio of 10, for example, is only 25% of the planar value. For pure intergranular fracture, the planar toughness $\mathcal{G}_c^{planar}$ is replaced by the boundary toughness $\mathcal{G}_c^b$, and assuming that no grain interlock behind the crack tip causes additional toughening, Equation 2 may be rewritten as

$$\mathcal{G}_c = \mathcal{G}_c^b(\mathcal{G}^{planar}/\langle\mathcal{G}\rangle) \quad (3a)$$

or

$$K_{Ic} = K_{Ic}^b(\mathcal{G}^{planar}/\langle\mathcal{G}\rangle)^{1/2} \quad (3b)$$

In order to estimate the boundary toughness of the as-received MgO which demonstrates 100% intergranular fracture, we consider the MgO grains to be equiaxed, i.e. having an aspect ratio of unity. From the measured toughness (Fig. 6) and Equation 3b we estimate $K_{Ic}^b = 1.87\,MPa\,m^{1/2}$. In earlier studies of MgO by Evans and Davidge [28], notched beam

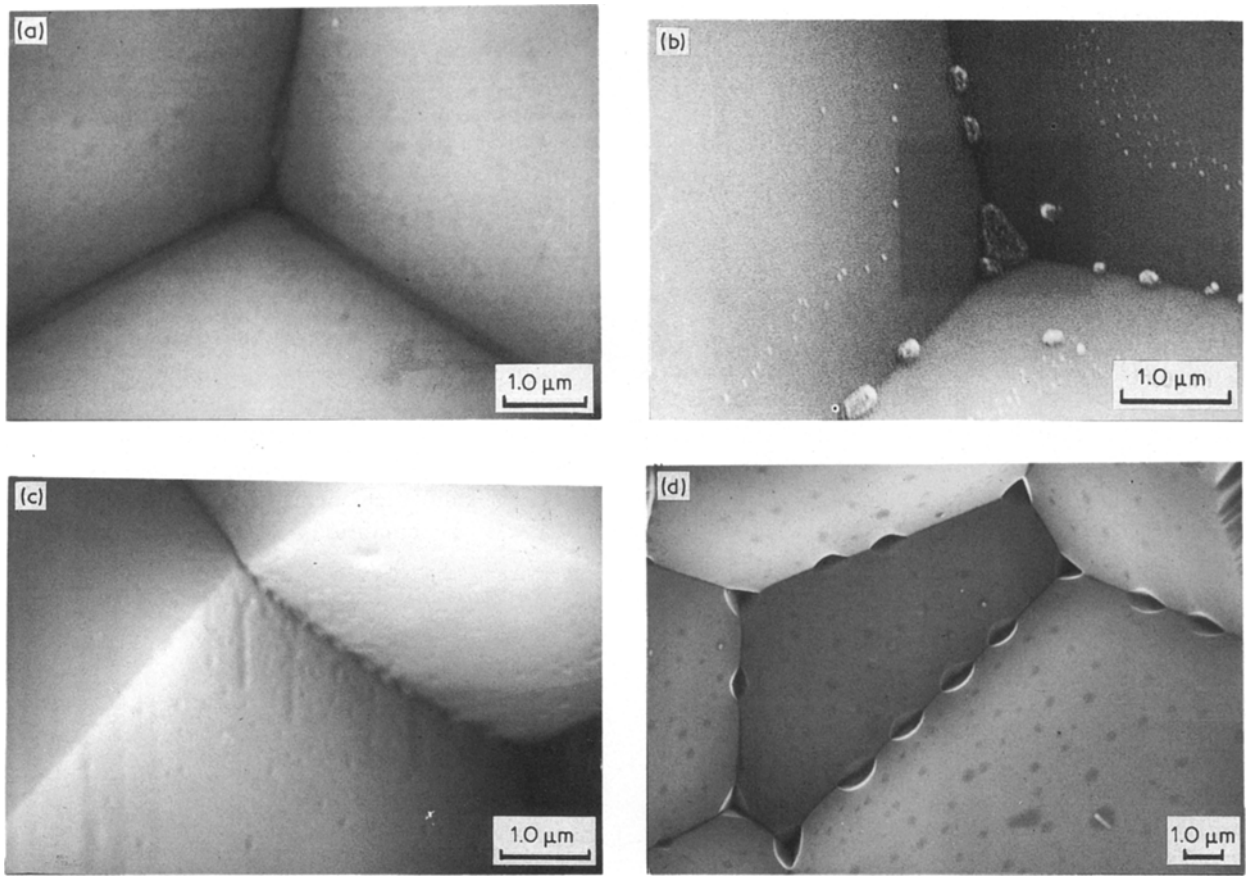

Figure 5 Scanning electron micrographs of fracture surfaces of MgO as a function of heat-treatment temperature. (a) As-received material contains continuous grain boundary film. (b) After 1250° C heat treatment, the interfacial film has broken up into isolated spheres. (c) Density of grain boundary spheres is reduced after first 1400° C heat treatment. (d) Grain boundary cavitation observed upon removal of grain boundary phase.

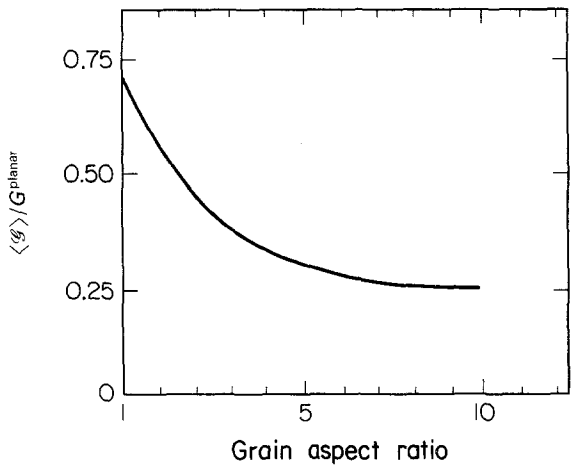

Figure 6 The relative crack driving force for intergranular fracture as a function of grain aspect ratio.

toughnesses were measured as a function of crack size. When the size of the crack approached the size of the microstructure (less than two grains) the measured toughness was 1.59 MPa $m^{1/2}$, while long intergranular cracks demonstrated toughnesses of 2.98 MPa $m^{1/2}$, slightly greater than our own measurement of 2.2 MPa $m^{1/2}$. The "short crack toughness" is expected to represent the boundary toughness, and shows reasonable agreement with our own estimates of K_{Ic}^{b}.

When fracture surfaces evidence both transgranular and intergranular morphology, the toughness is determined by both K_{Ic}^{b} and K_{Ic}^{g} in the following manner:

$$\mathcal{G}_c = \phi\, \mathcal{G}_c^{g} + (1 - \phi)\, \mathcal{G}_c^{b}(\mathcal{G}^{planar}/\langle \mathcal{G} \rangle) \quad (4a)$$

or

$$K_{Ic} = [\phi\, (K_{Ic}^{g})^2 + (1 - \phi)\, (K_{Ic}^{b})^2\, (\mathcal{G}^{planar}/\langle \mathcal{G} \rangle)]^{1/2} \quad (4b)$$

where ϕ represents the fraction of the crack front which experiences transgranular fracture, corrected for the increased crack front length due to intergranular fracture. Independent knowledge of the fracture toughness of single-crystal MgO or of the boundary toughness as lithium and fluorine are volatilized is required to solve Equation 4b. Our current observations do not allow for these calculations; none the less, the proposed model does offer some basis for comparison. If we assume that the boundary toughness approaches the grain toughness at the maximum value of K_{Ic} observed (2.9 MPa $m^{1/2}$), we then obtain a value for K_{Ic}^{g} of 2.6 Mpa $m^{1/2}$. Here we expect that K_{Ic}^{g} remains invariant with heat treatment since changes occur largely in the grain boundary phase.

The above model provides some insight into segregant-enhanced embrittlement in ceramic materials. While the inequality $K_{Ic}^{b} < K_{Ic}^{g}$ is necessary for grain boundary embrittlement, the necessary and sufficient conditions must include a term which represents the reduction in crack driving force, $\langle \mathcal{G} \rangle / \mathcal{G}^{planar}$. For embrittlement to occur, the following condition must be met:

$$K_{Ic}^{b} < (\langle \mathcal{G} \rangle / \mathcal{G}^{planar})^{1/2}\, K_{Ic}^{g} \quad (5)$$

Thus, the grain boundary toughness must be less than the grain toughness modified by the reduced crack driving force, suggesting that MgO grains must have a toughness K_{Ic}^{g} of at least 2.2 MPa $m^{1/2}$. Should the inequality be reversed, or $K_{Ic}^{g} < 2.2$ MPa $m^{1/2}$ for MgO, toughening will ensue.

5. Conclusions

For MgO which has been hot-pressed with LiF added as a sintering aid, the fracture behaviour is controlled by the presence of the second phase at the grain boundaries. By a series of heat treatments, the amount and configuration of the second phase is altered. Lithium and fluorine are volatilized and the continuous grain boundary phase is broken up. The resulting change in fracture behaviour manifests itself as an increase in fracture toughness and a decrease in the propensity for intergranular fracture.

Two competing processes occur during grain-boundary-controlled fracture. Crack growth along randomly oriented grain boundaries results in a decrease in the crack driving force, $\mathcal{G}$, and hence provides toughening. Alternatively, weakening of the grain boundary by impurity segregation may result in net embrittlement of the material. Conditions under which embrittlement or crack-deflection toughening will preferentially occur have been identified. Specifically, the decrease in crack driving force must be superseded by a decrease in grain boundary toughness relative to grain toughness for embrittlement to occur. In the MgO studied here, embrittlement of the grain boundaries due to the weak lithium- and fluorine-enhanced second phase dominates the effect of crack-deflection toughening.

Acknowledgements

This work was sponsored by the National Science Foundation under Grant No. DMR 8351476 and the National Science Foundation Materials Research Laboratory Grant No. DMR 841859.

References

1. J. H. WESTBROOK and D. L. WOOD, *Nature* **192** (1961) 1280.
2. C. J. McMAHON Jr, *Mater. Sci. Engng* **42** (1980) 215.
3. M. H. LEIPOLD, *J. Amer. Ceram. Soc.* **49** (1966) 498.
4. J. R. H. BLACK and W. D. KINGERY, *ibid.* **62** (1979) 176.
5. Y. M. CHIANG, A. F. HENRIKSEN and W. D. KINGERY, *ibid.* **64** (1981) 385.
6. H. L. MARCUS and M. E. FINE, *ibid.* **55** (1972) 568.
7. W. C. JOHNSON and D. F. STEIN, *ibid.* **58** (1975) 485.
8. A. W. FUNKENBUSCH and D. W. SMITH, *Metall. Trans.* **6A** (1975) 2299.
9. R. S. JUPP, D. F. STEIN and D. W. SMITH, *J. Mater. Sci.* **15** (1980) 96.
10. G. DeWITH and N. HATTU, *ibid.* **16** (1981) 841.
11. A. G. EVANS, D. GILLING and R. W. DAVIDGE, *ibid.* **5** (1970) 187.
12. R. W. RICE, *Proc. Br. Ceram. Soc.* **20** (1972) 329.
13. K. T. FABER and A. G. EVANS, *Acta Metall.* **31** (1983) 565.
14. *Idem, J. Amer. Ceram. Soc.* **66** (1983) C-94.
15. D. W. JOHNSON Jr., E. M. VOGEL and B. B. GHATE, in "Ferrites", edited by H. Watanabe, S. Iida and M. Sugimoto (Center for Academic Publications, Japan, 1980) p. 285.
16. G. K. BANSAL and A. H. HEUER, in "Fracture

Mechanics of Ceramics", Vol. 2, edited by R. C. Bradt, D. P. H. Hasselman and F. F. Lange (Plenum, New York, 1974) p. 677.
17. M. I. MENDELSON and M. E. FINE, *J. Amer. Ceram. Soc.* **57** (1974) 154.
18. R. W. RICE, *Proc. Br. Ceram. Soc.* **12** (1969) 99.
19. G. D. MILES *et al.*, *Trans. Br. Ceram. Soc.* **66** (1967) 319.
20. M. W. BENECKE, N. E. OLSON and J. A. PASK, *J. Amer. Ceram. Soc.* **50** (1967) 365.
21. P. E. HART, R. B. ATKIN and J. A. PASK, *ibid.* **53** (1970) 83.
22. P. CHANTIKUL *et al.*, *ibid.* **64** (1981) 539.
23. D. B. MARSHALL, T. NOMA and A. G. EVANS, *ibid.* **65** (1982) C-175.
24. J. M. HAUSSONNE *et al.*, *ibid.* **66** (1983) 801.
25. W. C. JOHNSON, D. F. STEIN and R. W. RICE, *ibid.* **57** (1974) 342.
26. L. NAVIAS, *ibid.* **19** (1936) 1.
27. B. HENDERSON and J. E. WERTZ, *Adv. Phys.* **17** (1968) 749.
28. A. G. EVANS and R. W. DAVIDGE, *Phil. Mag.* **20** (1969) 373.

Received 5 September 1988
and accepted 22 February 1989